A new feature extraction method and classification of early stage Parkinsonian rats with and without DBS treatment

B. Iravani, F. Towhidkhah & M. Roghani

Australasian Physical & Engineering Sciences in Medicine
The Official Journal of the Australasian College of Physical Scientists and Engineers in Medicine

ISSN 0158-9938

Australas Phys Eng Sci Med
DOI 10.1007/s13246-014-0296-3

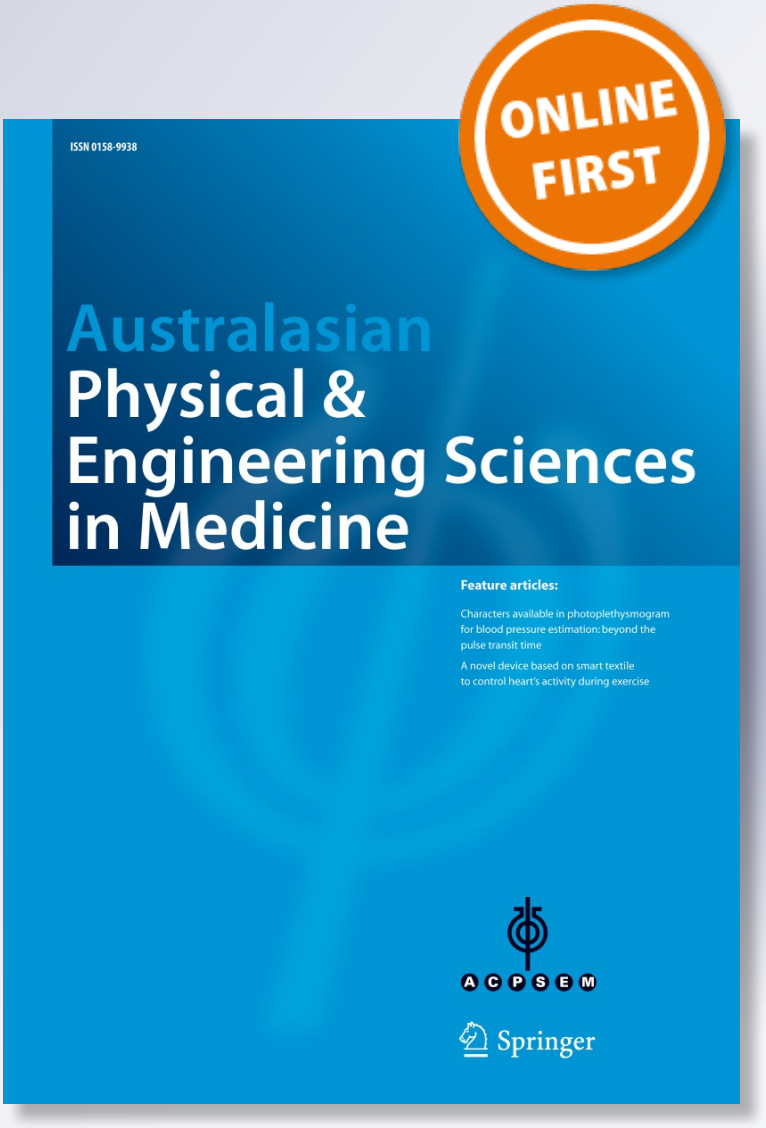

Springer

Australas Phys Eng Sci Med
DOI 10.1007/s13246-014-0296-3

SCIENTIFIC PAPER

A new feature extraction method and classification of early stage Parkinsonian rats with and without DBS treatment

B. Iravani · F. Towhidkhah · M. Roghani

Received: 12 November 2013 / Accepted: 25 August 2014

Abstract Parkinson Disease (PD) is one of the most common neural disorders worldwide. Different treatments such as medication and deep brain stimulation (DBS) have been proposed to minimize and control Parkinson's symptoms. DBS has been recognized as an effective approach to decrease most movement disorders of PD. In this study, a new method is proposed for feature extraction and separation of treated and untreated Parkinsonan rats. For this purpose, unilateral intrastriatal 6-hydroxydopamine (6-OHDA, 12.5 μg/5 μl of saline-ascorbate)-lesioned rats were treated with DBS. We performed a behavioral experiment and video tracked traveled trajectories of rats. Then, we investigated the effect of deep brain stimulation of subthalamus nucleus on their behavioral movements. Time, frequency and chaotic features of traveled trajectories were extracted. These features provide the ability to quantify the behavioral movements of Parkinsonian rats. The results showed that the traveled trajectories of untreated were more convoluted with the different time/frequency response. Compared to the traditional features used before to quantify the animals' behavior, the new features improved classification accuracy up to 80 % for untreated and treated rats.

Keywords Parkinson disease · 6-hydroxydopamine · Deep brain stimulation · Feature extraction · Behavioral movements · Classification

B. Iravani · F. Towhidkhah (✉)
Department of Biomedical, Amirkabir University of Technology, Hafez Street, Tehran, Iran
e-mail: Towhidkhah@aut.ac.ir

M. Roghani
Department of Physiology, School of Medicine, Shahed University, Tehran, Iran

Introduction

Parkinson's Disease (PD) is a progressive neural disorder which is characterized by an involuntary tremor, rigidity, bradykinesia (slowness of movement), unstable posture and difficulty in walking. PD is a disease of the Central Nervous System (CNS) which is caused by neurodegeneration of dopaminergic neurons in the basal ganglia. Currently, there are pharmacological and non-pharmacological treatments that only offer symptomatic relief for patients; however; they do not prevent neurodegeneration nor reverse the progression of this debilitating disease [1–3].

Deep brain stimulation (DBS) has been considered as significant progress in PD treatment since the discovery of levodopa as a superior anti-Parkinson drug in 1967 [4]. This treatment involves a stereotactic surgery which leads to implantation of stimulus electrodes. These electrodes stimulate specific deep brain nucleus. Among these nuclei, the subthalamic nucleus (STN) is a popular target for electrical stimulation and results in an anti-Parkinsonian effect. In 1993, the first DBS-STN was applied to treat disease. After a while, this treatment was adopted in treatment of other disorders like epilepsy, depression, chronic pain, and obsessive compulsive disorder [5–7].

Several studies have reviewed different approaches such as electrical [8–10] neuro-chemical [11, 12], and behavioral analysis to clarify the mechanisms of DBS [13, 14]; nevertheless, the mechanism of the DBS continues to remain obscure. Limitations in experimental techniques and complex responses of neurons to extracellular stimulations make it difficult to understand the precise effect of the DBS [15–18].

Since PD does not normally appear in animals, several methods have been proposed to produce neuropathological

Published online: 31 August 2014

of the human condition in laboratory animal [2]. The 6-hydroxydopamine (6-OHDA or Oxidopamine) model is the first animal model of PD that can reproduce the motor dysfunction of PD [19].This model can be achieved by injecting 6-OHDA directly into the dopaminergic system. The most common injecting site is median forebrain and striatum. The oxidative stress caused by the 6-OHDA destroys the dopaminergic neurons and produces 6-OHDA-induced PD in rats [3]. An injection of neurotoxin into the striatum leads to the early stage model of Parkinson. Depending on the stage of Parkinson, it may be required to apply one up to four injections [6].

Animals' behavioral movements are monitored in the studies as the reflection to the new treatment and medication methods. Therefore, having an effective method to study these movements is of a great importance.

Currently, a video tracking system is used for automation of behavioral experiments (Ethovision) [20]. In this system the behavioral movements of animal are captured through a video camera. These behavioral movements were analyzed and some features such as the average speed of locomotion or the distance between several individually identified animals are calculated. In addition, if certain regions are known as the region of interest (e.g., the center and edges of an open field) the proportion of time spent with the animals in those regions can also be calculated [20]. A drawback of this feature is that it has been not considered as a motor dysfunction specification associated with 6-OHDA induced neuronal damage [21].

One of the most common behavioral tests in the 6-OHDA model is rotational test resulted from imbalanced dopamine (DA) neural activities and the administration of apomorphine. The rate of rotation depends on the extent of disease induced in the rat [6]. In this test, an observer counts the ipsilateral and the contralateral rotations of the animals. This is a time consuming method specifically when the number of the rat increases. On the other hand, we can add the human error factor which may affect the reliability of the results. The aim of this paper is to present a computerized and automatic method to increase the speed of processing time as well as results reliability.

Our hypothesis is that using a combination of time, frequency, and chaotic features extracted from rat movements would be an efficient method to classify treated and untreated Parkinsonian rats. We investigated the effect of deep brain stimulation on apomorphine-induced rotational behavior of the rats. This method lends itself to develop an automatic approach to quantify the behavioral movements of treated and untreated Parkinsonian rats and follow up their treatment procedure.

Materials and methods

Animals

Adult male *Wistar* rats (260–330 g; $n = 14$) were housed in cages individually in temperature controlled colony room under normal light–dark cycles with free access to food and water. All rats were approximately in the same age range (10–12 weeks) and they were randomly divided into two groups. The first group, so-called lesion group, received a lesion in their nigrostriatal pathway to produce 6-OHDA-induced PD. No treatment procedure was applied to this group. The second group, so-called DBS group, received the same lesion but they were treated with deep brain stimulation. All experiments and animals' care were conducted in conformity with National Institutes of Health (NIH) and had been approved by the ethics of Shahed University Medical School (Tehran, Iran).

Surgical procedure

As mentioned before, in the present study, the 6-OHDA model was selected as the animal model for the PD. 6-OHDA neurotoxin does not cross the blood–brain barrier and classically injected directly into the target structure. Injecting 6-OHDA into the neostriatum can destroy DA neurons in the dopaminergic system and reproducing the pathological and behavioral changes of the PD in rodents [21].

For injecting a neurotoxin, rats were anaesthetized by 100 mg/kg ketamine and 5 mg/kg xilazine. Left lower quadrant of the abdomen was specified at the injection site of the anaesthetic. After rats became completely unconscious, they were placed on the stereotaxic apparatus (Stoelting, USA). The coordinates of injection site were: L −3 mm, AP +9.2 mm, V +4.5–5 mm from the center of the interaural line, according to the atlas of Paxinos and Watson [22]. After having the skull drilled carefully, single injection of 0.9 % saline containing 2.5 μg/μl of 6-hydroxydopamine-HCl (6-OHDA, Sigma) and 0.2 % ascorbic acid (w/v) at a rate of 1 μl/min was injected through a 5 μl Hamilton syringe in anaesthetized rats. The act of injecting performed in a slow rate (1 μl/min) to minimize the possibility of damaging brain tissue [3]. The rats were placed equally in two groups mentioned before.

Electrode implantation and stimulation

A bipolar home-made stimulating electrode was inserted stereotactically into the STN (L: 3 mm AP: −3.6 mm V: 8 mm relative to bregma) [22] in order to stimulate this nucleus.

Three days after operation (post-lesion), the DBS group was stimulated about 1 h per day for four continuous days. Too much stimulation duration may permanently damage the brain tissue; on the other hand the brief session of stimulation may be ineffective [23]. The parameters of stimulation were 100–130 Hz frequency, 100 μs pulse width and 100 μA current strength that were analogous to pervious experimental studies [9, 15–17, 24]. The strength of the current was determined to induce no involuntary movements in the animal [25].

Behavioral testing

A behavioral test was performed in both groups, 1 week after surgery. 2.5 mg/kg apomorphine hydrochloride (Sigma Chemical, St. Louis, MO, USA) was injected and they were placed in a cylinder with a diameter of 33 cm and height of 35 cm. The animals were allowed to habituate for 5 min and video tracked for about 15 min. Pattern of rotational behavior movements was recorded for later analysis. These videos were processed and the movement trajectory of rats was extracted.

Video processing for extracting trajectory

A passive marker was attached to the head of rats. It had a black color that made a good contrast with the body of the rats (see Fig. 1). Behavioral movements were video tracked by a SONY DSC-H70 camera with the frame rate of 29 fps and resolution 640 × 480 pixel for 15 min. The recorded videos were grayscaled and region of interest was determined. Only the inside of the cylinder was considered as the region of interest and the rest omitted. Only the marker was black in the region of interest. Since rats usually did not move a significant distance in 1/29th of a second, we reduced the sample rate to approximately three samples per second and the blackest pixel in each frame was found with a computer program and considered as the marker. The coordinates of the marker were stored in a matrix for later analysis. In some frames these coordinates

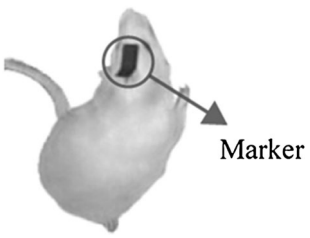

Fig. 1 The *black marker* attached to the head of rats to extract the traveled trajectory of them

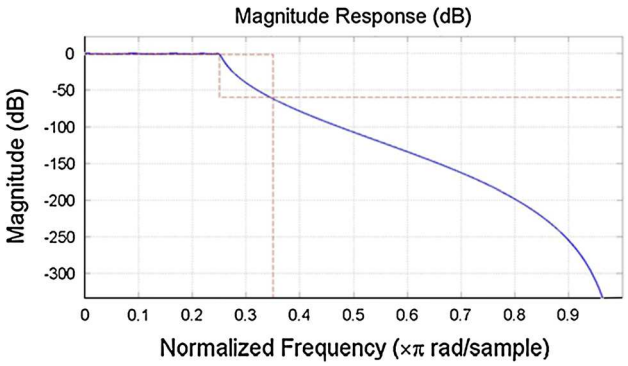

Fig. 2 Magnitude response of the low-pass filter to eliminate high frequency noise added to the signal

were determined incorrectly and made gaps in the trajectory signals. These gaps were detected and retrieved according to prior and post points by averaging.

Finally, we low-pass filtered the signal (9th order; FIR; cutoff frequency: 0.35π × rad/sample; zero phase distortion) to eliminate the high frequency noise that was added to the trajectory signal during the reading the coordinates of the marker. The magnitude response of this filter is illustrated in Fig. 2.

After filtering high frequency noise all trajectories were normalized as follows:

$$x_{\text{Normal}} = \frac{x - \frac{\max(x,y)+\min(x,y)}{2}}{\frac{\max(x,y)-\min(x,y)}{2}} \quad (1)$$

$$y_{\text{Normal}} = \frac{y - \frac{\max(x,y)+\min(x,y)}{2}}{\frac{\max(x,y)-\min(x,y)}{2}} \quad (2)$$

Inspired from neural networks application, the Eq. (2) is a mapping to normalize data set in order to set central point to zero, maximum value to 1, and minimum value to −1 without turning the average of data to zero.

Recorded videos of each rat were split into six parts with duration of 2.5 min and shuffled. This duration benefited enough information regarding the pathological behavior of rats. These parts were considered as independent and separated observations in order to provide a sufficient number of observations. Therefore, the total number of observations reached 84. The typical trajectory of each group is depicted in Fig. 3.

Feature extraction

In this section, various features were extracted to clearly differentiate between the two classes, i.e., lesion and DBS groups. To achieve this purpose, trajectory signals were analyzed in time, frequency and chaotic domains.

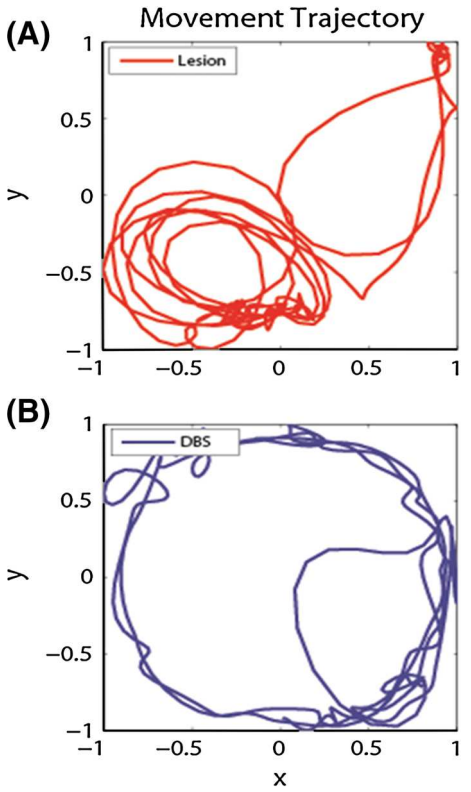

Fig. 3 Typical movement trajectory of rats. **a** Lesion, **b** DBS

Time-domain features

Time-domain features contain valuable information such as velocity and level of scattering. All rats had received apomorphine and hyperactivity was consequently expected. We investigate this phenomenon in this section. In this experiment the movement of rat was in a form of circular trajectories thus, polar coordinates were chosen for simplicity. Three key features of time-domain were analyzed: (1) variances of spatial amplitude (represented by x and y), (2) average and (3) variance of the phase (represented by θ) of the trajectory. These three features were calculated as shown in (3), (4) and (5).

$$\begin{bmatrix} \sigma_x^2 \\ \sigma_y^2 \end{bmatrix} = \begin{bmatrix} \int x^2 f(x)\mathrm{d}x - \mu_x^2 \\ \int y^2 f(y)\mathrm{d}y - \mu_y^2 \end{bmatrix} \tag{3}$$

$$\theta = \tan\left(\frac{y}{x}\right) \tag{4}$$

$$\begin{bmatrix} \mu_\theta \\ \sigma_\theta^2 \end{bmatrix} = \begin{bmatrix} \int \theta f(\theta)\mathrm{d}\theta \\ \int \theta^2 f(\theta)\mathrm{d}\theta - \mu_\theta^2 \end{bmatrix} \tag{5}$$

Frequency-domain features

Frequency-domain features were efficient in differentiating between lesion and DBS groups. Initially, we estimated the spectrum of trajectories by the Welch method [25]. Subsequently, we calculated the average power of the signal by using a rectangular approximation of the integral of the Power Spectrum Density as the first frequency-domain feature vector.

The DBS and lesion groups had different frequency responses since the lesion group's showed faster rotational behaviors compared to normal movements. In frequency domain, this represents greater energy in higher frequency bands (see Fig. 4). To calculate the frequency responses of the groups, the fast Fourier transform was applied. Two frequency bands were defined for a better comparison: from 0 to 0.1 Hz and from 0.1 to 0.2 Hz. We calculated sum of energy in these intervals as the next frequency-domain feature vector.

Chaotic feature investigation

In the first place, we investigated whether trajectories signals were chaotic or not. The most useful dynamical diagnosis parameter for chaotic system is Lyapunov exponent which measures the divergence of nearby trajectories [5, 26]. The largest Lyapunov exponent was estimated by Jacobian approach [27].

If the average Lyapunov exponent of a system is positive, then the behavior of that system will be chaotic [5].

Determining the minimum embedding dimension and maximum delay

The Cao's method was used to specify the minimum embedding dimension [28, 29]. In this method, the quantity $E_1(d)$ was computed by (6)

$$E_1(d) = \frac{E(d+1)}{E(d)} \tag{6}$$

where $E(d)$ was driven by (7) and d is the embedding dimension. For d larger than d_0, $E_1(d)$ is constant and the minimum embedding dimension would be equal to d_0.

$$E(d) = \frac{1}{N - \mathrm{d}\tau} \sum_{i=l}^{N-dr} a2(i,d) \tag{7}$$

$$a_2(i,d) = \frac{||Y_i(d+1) - Y_{n(i,d)}(d+1)||}{||Y_i(d) - Y_{n(i,d)}(d)||} \tag{8}$$

where ||.|| in (8) is the Euclidean distance and determine by (9):

$$Y_k(m) - Y_l(m) = \max|x_{k+j\tau} - x_{l+j\tau}| \quad 0 \le j \le m-1 \tag{9}$$

For an arbitrary time series x_1, x_2, x_3,…,x_n, the time delay vector is defined as follows:

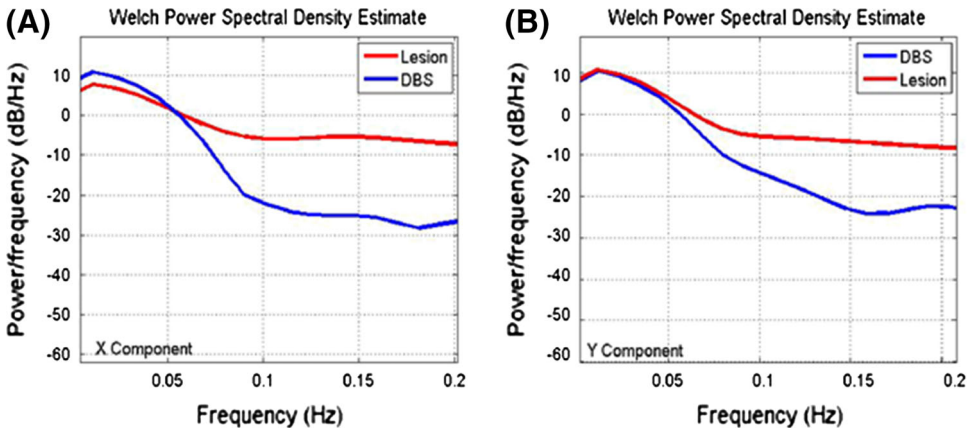

Fig. 4 Typical Welch power spectrum density. **a** Power spectrum density of x component, **b** power spectrum density of y component

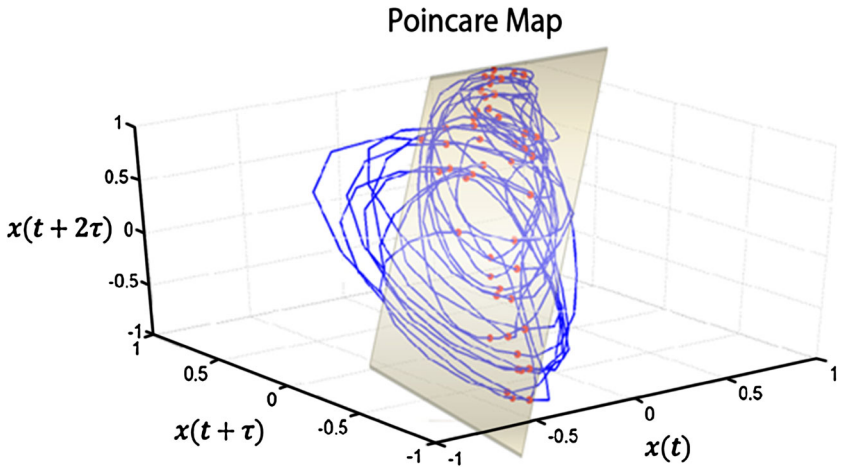

Fig. 5 Poincare section plane of travel trajectories in 3D phase space. The intersection of the plane with the attractors resulted in a cluster of hit points (d = 3 and τ = 3)

$$Y_i(d) = [x_i, x_{i+\tau}, \ldots, x_{i+(d-1)\tau}] \quad i = 1, 2, \ldots, N - (d-1)\tau \tag{10}$$

$Y_i(d+1)$ is the ith reestablished vector with embedding dimension $d+1$. $Y_{n(i,d)}$ is the nearest neighbor of $Y_i(d)$ in the d-dimensional reconstructed phase space [29]. We computed $E_1(d)$ and the average of d_0 was derived about three for the trajectories.

The other key parameter is the maximum delay which was determined experimentally. Theoretically, there is no limitation on selecting the time delay. We estimated the maximum delay by using a first local minimum of mutual information.

Chaotic features

For chaotic features analysis, we depicted phase space in a three dimensional format using the minimum embedding dimension and maximum delay computed in the previous section.

The Poincare map is typically a tool to analyze dynamic systems [30]. We applied it to extract chaotic distinction of lesion and DBS groups. To do this, we determined a proper surface as Poincare section. We chose a plane which was perpendicular to the attractors and consequently had maximum intersections with the attractors. This plane with normal vector 0.39 a_x + 0.47 a_y − 0.8 a_z and point (0, 0, 0) was depicted in the phase space in Fig. 5. Intersection attractors with the plane resulted in a cluster of hit points. The statistical characteristics of Poincare hit points, including averages and variances of points and their distances, were considered as the primary chaotic features.

The fractal dimension is a technique to measure the convolutedness of a waveform [31]. There are several methods to estimate fractal dimension. The Katz method was applied to estimate the fractal dimension and added as another chaotic feature that was derived directly from movement signals in the time domain as follows [32]:

$$D = \frac{\log_{10}(L)}{\log_{10}(d)} \tag{11}$$

where L in (11) is the total curve length and d is the maximum distance between the first point and the rest points of the curve and it derives from (12)

$$d = \max(\text{distance}(1, i)) \quad (12)$$

The fractal dimension is highly dependent to the unit of measurement. For solving this problem, the distances between points were normalized by dividing them by the average distance between successive points [32].

$$D = \frac{\log_{10}(L/a)}{\log_{10}\left(d/a\right)} \quad (13)$$

In fact, fractal dimension compares the numbers of segments of a curve with the minimum number that is really needed for constructing that curve.

Finally, introduced feature vectors were calculated we statically analyse them using the Wilcoxon single rank test to compare two groups. This test is a non-parametric analysis, which can be used as an alternative to the paired student's t test.

Classification

To classify rats in lesion and DBS groups by means of mathematical tools we applied extracted features to three classifiers including K-nearest neighborhood (KNN), Bases Quadratic, and Neural Network classifiers. The classification errors were calculated and the best one was chosen as the final classifier.

We split database into two parts. The first part consisting of 60 % of whole data was applied in the training phase and the rest of it was used in the test phase.

KNN classifier

As the first classifier, KNN was used to separate the two groups of rats. In this classifier the value of K is required to determine. A higher value of K increases robustness of the classifier to noise, however, it produces a fuzzy separation boundary. A lower value of K decreases the classifier robustness and produces a crisp separation boundary. We set K to three to obtain a good tradeoff between noise resistance and boundary fuzziness. The process of classifying has performed for twenty times and the average accuracy was reported as the final result.

Bayes quadratic classifier

This classifier separates measurements of two or more classes of objects/events by a quadratic surface [33]. Similar to KNN classifier, in this case the classification was performed twenty times and the average accuracy was recorded, as well.

Neural network classifier

The neural network (NN) was the last classifier applied to the experimental data. We used a single layer feed-forward fully connected network (see Fig. 6) trained by backpropagation [34]. The hidden layer includes 15 neurons, the number of neurons in the input layer was equal to feature vectors and two neurons in the output layer representing two (i.e., lesion and DBS) groups. The neuron with higher value determined the winner group.

Results

Feature vectors

As mentioned before we investigated whether the introduced features were able to present a meaningful difference between the path shape of travel of lesion and DBS groups and to classify the rats to treated and untreated.

We performed the Wilcoxon single-rank test to verify that the differences occurred in the features were meaningful. Moreover, the classification was accomplished using these features to show that they were beneficial to detect treated rats from untreated ones. The results of all 14 rats are shown in Table 1.

Some of these features were significantly different in two groups (Wilcoxon, $P < 0.05$) including the x component of the sum of the energy in band 1, both components (x, y) of the sum of the energy in band 2, both components (x, y) of the average of Poincare hit points, the y component of the variance of Poincare hit points, and the x component of the average of the distance between successive points.

The x component of the average of variance of spatial amplitude in the lesion group ($mean \pm SEM$: $0.0065 \pm 3.3 \times 10^{-5}$, $n = 42$) was 51 % greater than that of the DBS group ($mean \pm SEM$: $0.0043 \pm 1.5 \times 10^{-5}$, $n = 42$). In addition, the average of the variance of the polar phase (θ) was 30 % greater in lesion group ($mean \pm SEM$: $0.0536 \pm 6 \times 10^{-4}$, $n = 42$) than that of the DBS group ($mean \pm SEM$: $0.0429 \pm 8 \times 10^{-5}$, $n = 42$).

The variances of the x and y components of the sum of the energy in band 1 in the lesion group ($mean \pm SEM$ *of* x *component*, $mean \pm SEM$ *of* y *component*: 22.44 ± 100.15, 25.82 ± 169.5, $n = 42$) were 40 % and 15.3 % smaller than those of the DBS group ($mean \pm SEM$ *of* x *component*, $mean \pm SEM$ *of* y *component*: 29.25 ± 168.25, 27.58 ± 199.93, $n = 42$) respectively.

The averages of x and y components of the sum of the energy in band 2 in lesion group ($mean \pm SEM$ *of* x *component*, $mean \pm SEM$ *of* y *component*: 3.4351 ± 14.32,

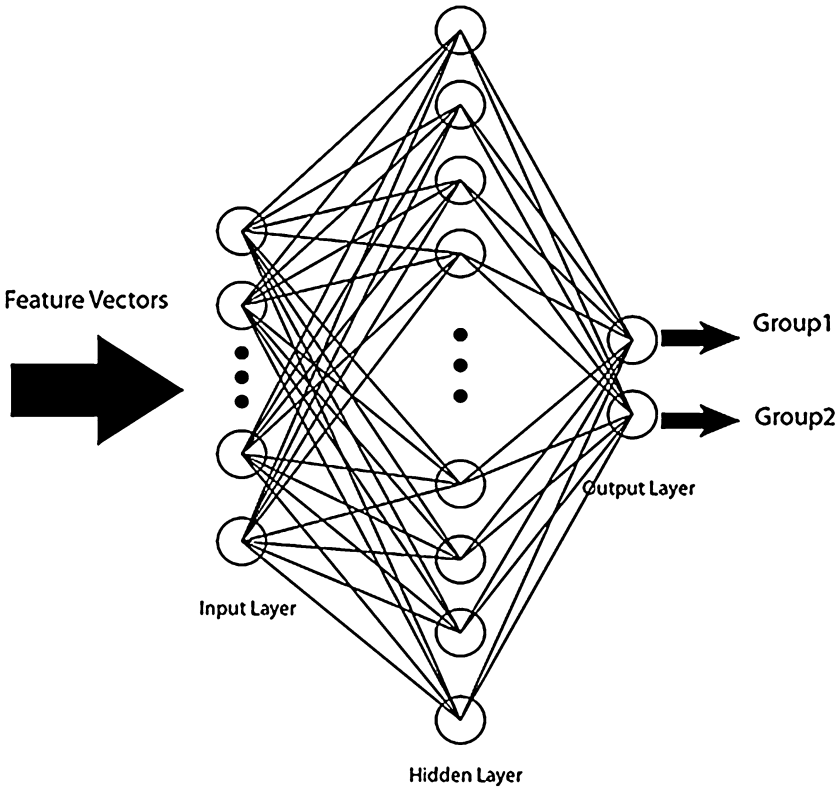

Fig. 6 Neural network classifier. The input of the network is the feature vectors and the output is the classes (i.e., lesion and DBS)

2.9031 ± 11.06, $n = 42$) were 50 and 13 % greater than those of DBS group (1.3637 ± 2.076, 1.3633 ± 3.54, $n = 42$), respectively.

The average of the distance between successive Poincare hit points of the x component in the lesion group (*mean* ± *SEM*: 0.8544 ± 0.1308, $n = 42$) was 19 % greater than that of the DBS group (*mean* ± *SEM*: 0.6901 ± 0.2466, $n = 42$).

In addition to above outcomes, we observed that, during the stimulation, rats were highly sensitive to the surrounding sounds. Unlike the lesion group the DBS group did not show any significant rotational behavior.

Classification

We extracted time, frequency, and chaotic features of behavioral movements and applied them to the classifiers. These classifiers including KNN, Quadratic, and Neural Network (NN) classifiers classified the rats into treated and untreated groups (lesion-DBS). The accuracy results of classifying are depicted in Fig. 7.

As it is obvious, the NN classifier shows the highest test-accuracy (80 %) compared to the others, thus, it was chosen as the final classifier.

Discussion

It is important to remember that the main aim of this research is to present a new method and features to quantify and analyze the behavioral movements of the Parkinsonian rats. The results show a good capability of suggested time, frequency, and chaotic features to classify treated and untreated Parkinsonian rats.

A problem in the traditional manual method to study the rat movement is that in the mild stage of the disease the rat movement misbehavior is not simply detectable. The method proposed in this paper can be used to facilitate the detection of mild disease stage.

We used a mild (one lesion) striatal lesion rat PD model in this study which was established by Kirik [35]. We applied small and fixed stimulation strength while in other studies the stimulation strength was selected to maximize the behavioral improvements (75–200 μA). Choosing such a low strength would minimize the possibility of current spreading to the adjacent structures. Applying high strength would obscure the pure effect of STN-DBS by electrical stimulating of surrounding structures [6]. We observed the behavioral improvements occurred in most rats in the DBS group by STN-DBS with the current strength of 100 μA.

There is a possibility that the insertion of electrodes into STN causes a mechanical injury or an electrical injury caused by the high frequency stimulations of STN improves the motor behaviors. To investigate the impact of insertion of electrodes we inserted an electrode stereotactically into the STN of a rat. This specific rat did not receive any stimulation. The behavioral testing showed that no therapeutic effect was obtained by inserting the

Table 1 Results in detailed obtained from time/frequency and chaotic analysis

Feature	Group			
	Lesion *Mean ± SEM*	DBS *Mean ± SEM*	Wilcoxon-test *P value*	Feature domain
Variance of spatial amplitude *x*-component	$0.0065 \pm 3.3 \times 10^{-5}$	$0.0043 \pm 1.5 \times 10^{-5}$	0.074	Time domain feature
Variance of spatial amplitude *y*-component	$0.0054 \pm 2.17 \times 10^{-5}$	$0.0058 \pm 3.88 \times 10^{-5}$	0.645	
Average of polar phase (θ)	0.7518 ± 0.0136	0.7951 ± 0.027	0.1615	
Variance of polar phase (θ)	$0.0536 \pm 6 \times 10^{-4}$	$0.0429 \pm 8 \times 10^{-5}$	0.125	
Average of power spectrum density *x*-component	0.2966 ± 0.0082	0.3512 ± 0.017	0.07577	Frequency domain feature
Average of power spectrum density *y*-component	0.3285 ± 0.0171	0.3359 ± 0.0167	0.6643	
Sum of energy (band.1) *x*-component	22.44 ± 100.15	29.25 ± 168.25	0.028	
Sum of energy (band.1) *y*-component	25.82 ± 169.5	27.58 ± 199.93	0.5224	
Sum of energy (band.2) *x*-component	3.4351 ± 14.32	1.3637 ± 2.076	0.0073	
Sum of energy (band.2) *y*-component	2.9031 ± 11.06	1.3633 ± 3.54	0.0091	
Average Poincare hit points *x*-component (x_x, y_x)	$(0.068 \pm 0.1171, -0.011 \pm 0.0016)$	$(0.089 \pm 0.17, -0.0089 \pm 0.0021)$	0.0084	Chaotic feature
Average Poincare hit points *y*-component (x_y, y_y)	$(0.0878 \pm 0.1519, -0.0120 \pm 0.002)$	$(0.0298 \pm 0.1748, -0.0029 \pm 0.0022)$	0.0025	
Variance Poincare hit points *x*-component	$(0.84 \pm 0.1080, 0.0080 \pm 1.33 \times 10^{-5})$	$(0.8654 \pm 0.2423, 0.01 \pm 1.92 \times 10^{-5})$	0.0934	
Variance Poincare hit points *y*-component	$(0.087 \pm 0.159, 0.0298 \pm 0.1784)$	$(-0.0120 \pm 0.0020, -0.0029 \pm 0.022)$	0.0475	
Average distance between successive Poincare hit points *x*-component	0.8544 ± 0.1308	0.6901 ± 0.2466	0.0217	
Variance distance between successive Poincare hit points *x*-component	0.5109 ± 0.1253	0.4592 ± 0.2073	0.2359	
Average distance between successive Poincare hit points *y*-component	0.8321 ± 0.1286	0.6031 ± 0.1224	0.7781	
Variance distance between successive Poincare hit points *y*-component	0.5388 ± 0.2033	0.4196 ± 0.1979	0.2358	
Katz Fractal dimension *x*-component	1.84 ± 0.1219	1.74 ± 0.1124	0.1063	
Katz Fractal dimension *y*-component	1.8060 ± 0.0991	1.7469 ± 0.1595	0.2810	

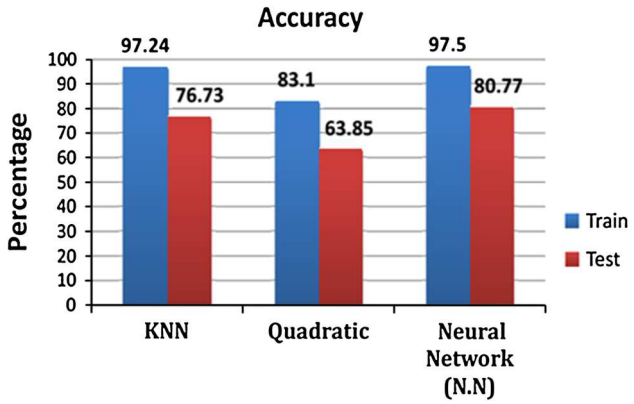

Fig. 7 Accuracy of classifiers

electrodes without stimulation. The other studies also assumed that mechanical injuries did not alter the results [6].

Hranck et al. result shows that high frequency stimulation more than 4 h can cause damage to neurons. Because the duration of stimulation in this study was less that 1 h per day, there is no electrical stimulation injury [36].

Few researchers have studied the path shape of travel in rats. Yaski et al. investigated the effect of global geometry of the environment on the path shape of travel in rats. Their result shows that environment has a great impact on exploration and navigation of rats. [37] Barun et al. reported that both route-based and spatial navigation are affected by depletion of DA in dorsal striatal [38].

Several behavioral tests have been proposed to investigate the effect of STN-DBS. The present study offered an automate process to study the therapeutic effect of STN-DBS and an unsupervised record of the rats' traveled trajectories. The introduced features extracted and compared by our computer program was appropriate to be used to reveal the effect of STN-DBS. Furthermore, Our method may even be used for other treatments in the future too.

We found that the DBS affected the path shape travel of Parkinsonian rats and it was more discernible in a horizontal direction (x-component). The suggested time and frequency features (i.e., the average variance of spatial amplitude, the variance of the polar phase, and average energy) offered that lesion group had higher activity than the DBS group caused by the pathological rotational behavior. In the other words, the DBS reduced the PD's symptoms in rats, and it was detectable by our introduced features.

In addition, the chaotic features (i.e., average of the Katz fractal dimension) showed that the lesion group had more complex path shape of travel than the DBS group. This complexity is result of pathological rotational behavior of the rats in lesion group.

Since the rats in the DBS group did not show apomorphine-induced rotational behavior; it can be concluded that the imbalance of dopamine in nigrostriatal has been regulated due to the stimulation and it improved the motor impairments that are in conformity with the previous studies [6, 17, 18, 24, 25]. An improvement of cognitive behavior also reported by Temel and Desbonnet. Their results showed that the bilateral electrical stimulation frequency of 130 Hz, 60 μs in duration, 3 and 30 μA in strength improved cognitive behavior. [16, 18].

In conclusion, we find that the Parkinsonian rats had different time/frequency-domain and chaotic features. Our results showed that using the presented feature vectors benefits the classification of rats to the treated and untreated groups with the acceptable accuracy.

To summarize, in this study we performed an experiment and video tracked behavioral movements of STN-DBS treated and untreated Parkinson rats. We defined and analysed the time/frequency-domain and chaotic features of the traveled movements and classify them into the lesion and DBS groups by a NN classifier with the accuracy of 80 %. This study offered an automatic method to classify rats and a mathematical tool to analysis their behaviors that it would be useful for further experimental behavioral studies of Parkinsonian rats under different treatment methods.

References

1. Singh N, Pillay V, Choonara YE (2007) Advances in the treatment of Parkinson's disease. Prog Neurobiol 81:29–44
2. Sauer H, Oertel WH (1994) Progressive degeneration of nigrostriatal dopamine neurons following intrastriatal terminal lesions with 6-hydroxydopamine: a combined retrograde tracing and immunocytochemical study in the rat. Neuroscience 59:401–415
3. Roghani M, Niknam A, Jalali-Nadoushan MR, Kiasalari Z, Khalili M, Baluchnejadmojarad T (2010) Oral pelargonidin exerts dose-dependent neuroprotection in 6-hydroxydopamine rat model of hemi-Parkinsonism. Brain Res Bull 82:279–283
4. Hornykiewicz O (2010) A brief history of levodopa. J Neurol 257:249–252
5. Razlighi MS, Jafari AH, Firoozabadi SM, Shahidi GA (2012) Study of chaotic behavior of tremor of some Parkinsonians under deep brain stimulation. Australas Phys Eng Sci Med 35:25–30
6. Fang X, Sugiyama K, Akamine S, Namba H (2006) Improvements in motor behavioral tests during deep brain stimulation of the subthalamic nucleus in rats with different degrees of unilateral Parkinsonism. Brain Res J 1120:202–210
7. Silberstein P, Bittar RG et al (2009) Deep brain stimulation for Parkinson's disease: Australian referral guidelines. J Clin Neurosci 16:1001–1008
8. Hashimoto T, Elder CM, Okun MS, Patrick SK, Vitek JL (2003) Stimulation of the subthalamic nucleus changes the firing pattern of pallidal neurons. J Neurosci 23:1916–1923
9. Maesawa S, Kaneoke Y, Kajita Y, Usui N, Misawa N, Nakayama A, Yoshida J (2004) Long-term stimulation of the subthalamic

nucleus in hemiParkinsonian rats: neuroprotection of dopaminergic neurons. J Neurosurg 100:679–687
10. Nambu A, Tokuno H, Takada M (2002) Functional significance of the cortico–subthalamo–pallidal 'hyperdirect', pathway. Neurosci Res 43:111–117
11. Windels F, Kiyatkin EA (2003) Modulatory action of acetylcholine on striatal neurons: microiontophoretic study in awake, unrestrained rats. Eur J Neurosci 17:613–622
12. Windels F, Bruet N, Poupard A, Urbain N, Chouvet G, Feuerstein C, Savasta ME (2000) Effects of high frequency stimulation of subthalamic nucleus on extracellular glutamate and GABA in substantia nigra and globus pallidus in the normal rat. Eur J Neurosci 12:4141–4146
13. McIntyre CC, Savasta M, Goff LK-L, Vitek JL (2003) Uncovering the mechanism(s) of action of deep brain stimulation: activation, inhibition, or both. Clin Neurophysiol 115:1239–1248
14. Shah RS, Chang SY, Min HK et al (2010) Deep brain stimulation: technology at the cutting edge. J Clin Neurol 6(4):167–182
15. Chang JY, Shi LH, Luo FK, Woodward DJ et al (2003) High frequency stimulation of the subthalamic nucleus improves treadmill locomotion in unilateral 6-hydroxydopamine lesioned rats. Brain Res 983(1–2):98–106
16. Desbonnet L, Temel Y, Visser-Vandewalle V et al (2004) Premature responding following bilateral stimulation of the rat subthalamic nucleus is amplitude and frequency dependent. Brain Res 1008(2):198–204
17. Shi LH, Woodward DJ, Luo FK et al (2004) High-frequency stimulation of the subthalamic nucleus reverses limb-use asymmetry in rats with unilateral 6-hydroxydopamine lesions. Brain Res 1013:98–106
18. Temel Y, Visser-Vandewalle V, Aendekerk B et al (2005) Acute and separate modulation of motor and cognitive performance in parkinsonian rats by bilateral stimulation of the subthalamic nucleus. Exp Neurol 193:43–52
19. Rahimi F, Typlt M, Jog MS (2011) Levodopa and Parkinson disease—electrophysiological perspectives in animal models. Exp Neurol 231:11–13
20. Noldus LP, Spink AJ, Tegelenbosch RA (2001) EthoVision: a versatile video tracking system for automation of behavioral experiments, behavior research methods. Instrum Comput 33(3):398–414
21. Blandini F, Armentero MT, Martignoni E (2008) The 6-hydroxydopamine model: news from the past. Parkinsonism Relat Disord 14:124–129
22. Paxinos G, Watson C (1986) The rat brain in stereotaxic coordinates, 2nd edn. Academic, San Diego
23. Harnack D, Winter C, Meissner W et al (2004) The effects of electrode material, charge density and stimulation duration on the safety of high frequency stimulation of subthalamic nucleus in rats. J Neurosci Method 138(1–2):207–216
24. Darbaky Y, Forni C, Amalric M, Baunez C (2003) High frequency stimulation of the subthalamic nucleus has beneficial antiparkinsonian effects on motor functions in rats, but less efficiency in a choice reaction time task. Eur J Neurosci 18(4):951–956
25. Creed M, Hamani C, Nobrega JN (2011) Deep brain stimulation of the subthalamic or entopeduncular nucleus attenuates vacuous chewing movements in a rodent model of tardive dyskinesia. Eur Neuropsychopharmacol 21(5):393–400
26. Welch P D (1967) The use of fast Fourier transform for estimation of power spectra: a method based on time averaging over short modified periodogram. IEEE Trans Audio Electroacoust AU-15:70–73
27. Wolf A, Swift JB et al (1985) Determining Lyapunov exponent from a time series. Phys D: Nonlinear Phenom 16(3):258–317
28. Lai D, Chen G (1998) Statistical analysis of Lyapunov exponents from time series: a Jacobian approach. Math Comput Model 27(7):1–9
29. Cao L (1997) Practical method for determining the minimum embedding dimension of a scalar time series. Phys D: Nonlinear Phenom 110(1–2):43–50
30. Frazier C, Kockelman KM (2004) Chaos theory and transportation systems: an instructive example. Transp Res Rec 1897:9–17
31. Parker TS, Chua LO (1987) Chaos: a tutorial for engineers. Proc IEEE 75(8):982–1008
32. Katz MJ (1988) Fractals and the analysis of waveforms. Comput Biol Med 18(3):145–156
33. Esteller R, Vachtsevanos G, Echauz J, Litt B (2001) Comparison of waveform fractal dimension algorithms. IEEE Trans Circ Syst I: Fundam Theor Appl 48(2):177–183
34. Duda RO, Hart PE, Stork DG (2001) Pattern classification, 2nd edn. Wiley, New York
35. Rumelhart DE, Hinton GE, Williams RJ (1986) Learning internal representations by error propagation. In Rumelhart DE (ed) Parallel distributed processing: explorations in the microstructure of cognition, vol 1, pp 318–362. MIT Press, Cambridge, MA
36. Kirik D, Rosenblad C, Bjorklund A (1998) Characterization of behavioral and neurodegenerative changes following partial lesions of the nigrostriatal dopamine system induced by intrastriatal 6-hydroxydopamine in the rat. Exp Neurol 152:259–277
37. Harnack D, Winter C, Meissner W, Reum T, Kupsch A, Morgenstern R (2004) The effects of electrode material, charge density and stimulation duration on the safety of high-frequency stimulation of the subthalamic nucleus in rats. J Neurosci Method 138:207–216
38. Yaski O, Portugali J, Eilam D (2011) Arena geometry and path shape: when rats travel in straight or in circuitous paths? Behav Brain Res 225:449–454
39. Braun A, Graham D, Schaefer T, Vorhees C, Williams V (2012) Dorsal striatal dopamine depletion impairs both allocentric and egocentric navigation in rats. Neurobiol Learn Mem 97:402–408